Electronic Supplementary Material (ESI) for Inorganic Chemistry Frontiers.


# Supporting Information

## Tin Nanoparticles Embedded in N-Doped Microporous Carbon Matrix Deriving from ZIF-8 as Anode for Ultralong-life and Ultrahigh-rate Lithium-Ion Batteries

Qingqing Han,[a] Ting Jin,[a] Yang Li,[a] Yuchang Si,[*b] Haixia Li,[*a] Yijing Wang[a] and Lifang Jiao[*a]

[a]Key Laboratory of Advanced Energy Materials Chemistry (Ministry of Education), College of Chemistry, Nankai University, Tianjin 300071, China.

E-mail: jiaolf@nankai.edu.cn.

[b]Logistics University of People's Armed Police Force

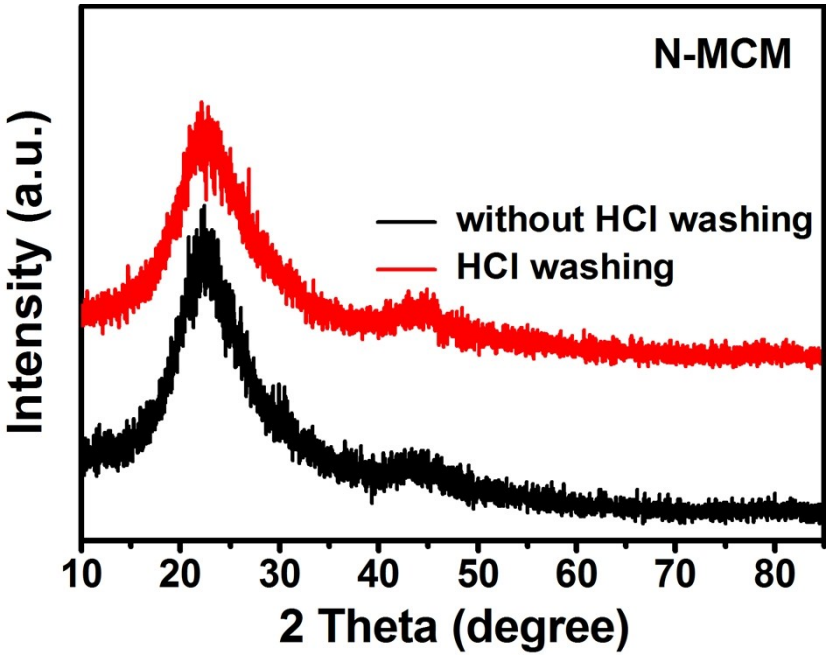


**Fig. S1.** XRD patterns of nitrogen-doped microporous carbon matrix (N-MCM) before and after treated with HCl.

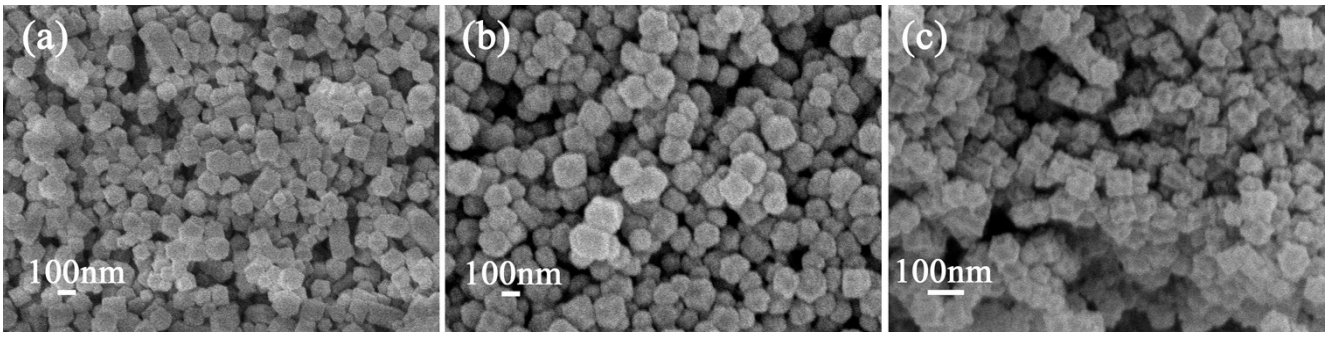


**Fig. S2.** SEM images of (a) ZIF-8, (b) nitrogen-doped microporous carbon matrix (N-MCM) and (c) Sn@N-MCM obtained at 600 °C.

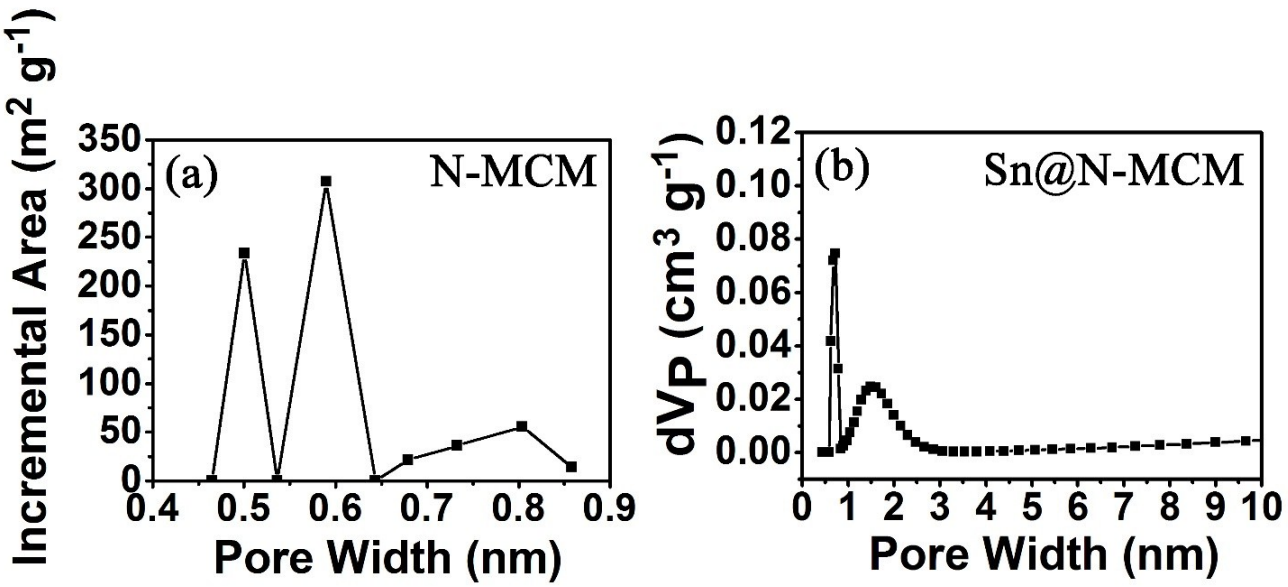


**Fig. S3.** Pore size distribution curves of (a) N-MCM and (b) Sn@N-MCM.

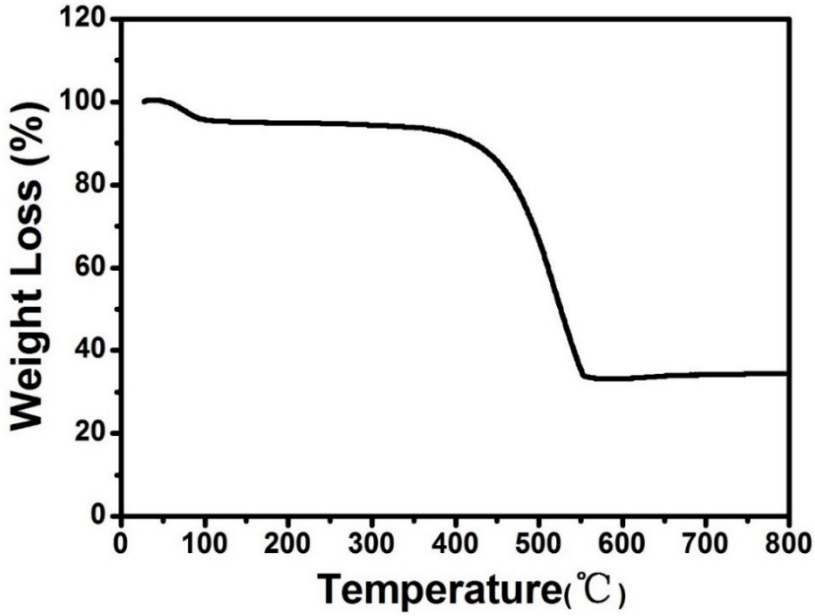


**Fig. S4.** TGA curve of Sn@N-MCM in air with a heating rate of 5 °C $min^{-1}$.

The decline of the curve below 100 °C can be attributed to the loss of moisture in the sample. The fast weight loss occurred between 350 °C and 550 °C, which is ascribed to the carbon combustion ($C + O_2 \rightarrow CO_2$ (gas)). The Sn content was calculated following equation (1):

$$\mathrm{Sn\ (wt\%)} = 100 \times \frac{\text{molecular weight of Sn}}{\text{molecular weight of } SnO_2} \times \frac{\text{final weight}}{\text{initial weight}} \qquad (1)$$

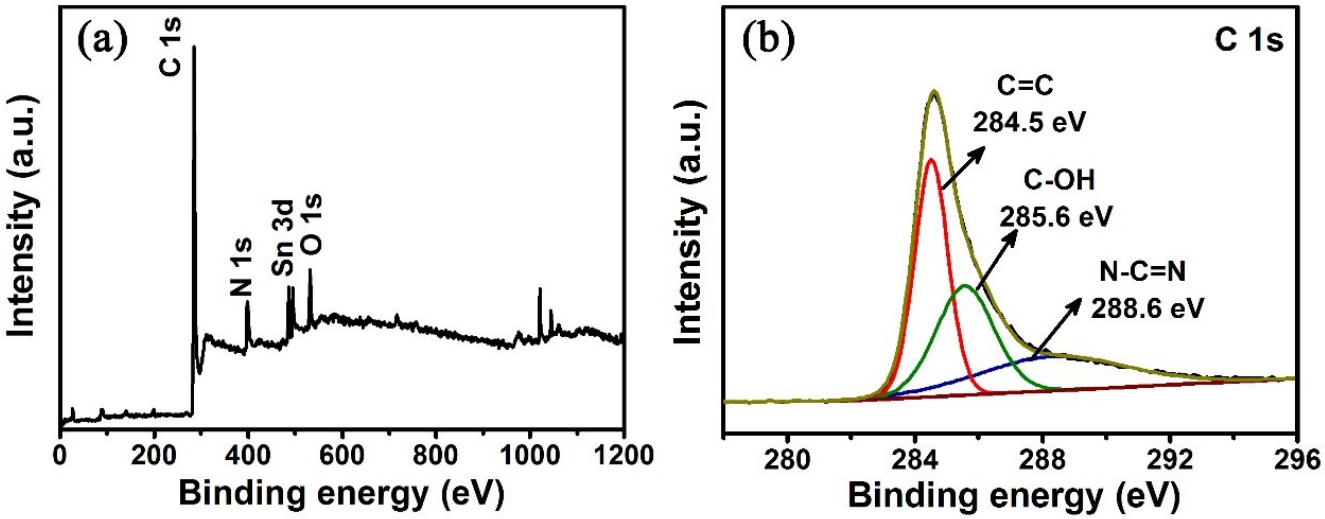


**Fig. S5.** XPS spectra of Sn@N-MCM (a) Full spectrum and (b) high resolution C 1s spectrum.

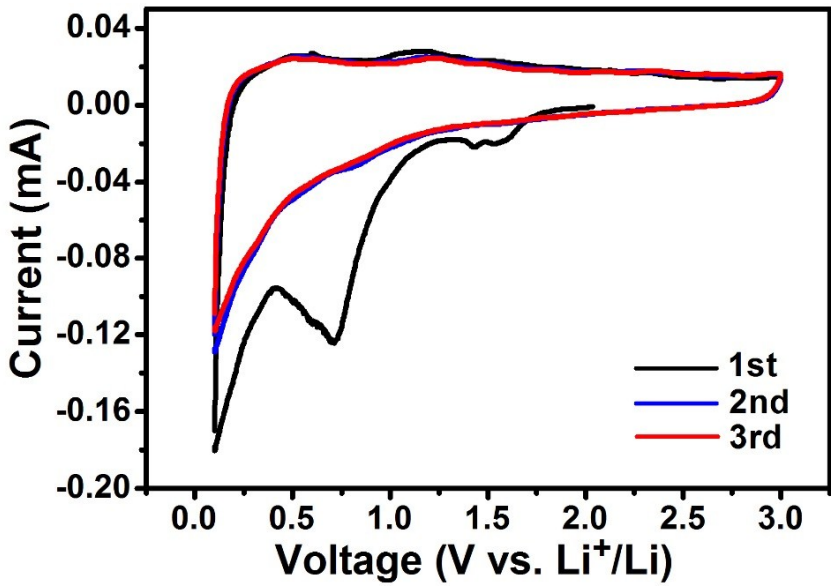


**Fig. S6.** Cyclic voltammetry curves of Sn@N-MCM scanned at a rate of 0.1 mV $s^{-1}$.

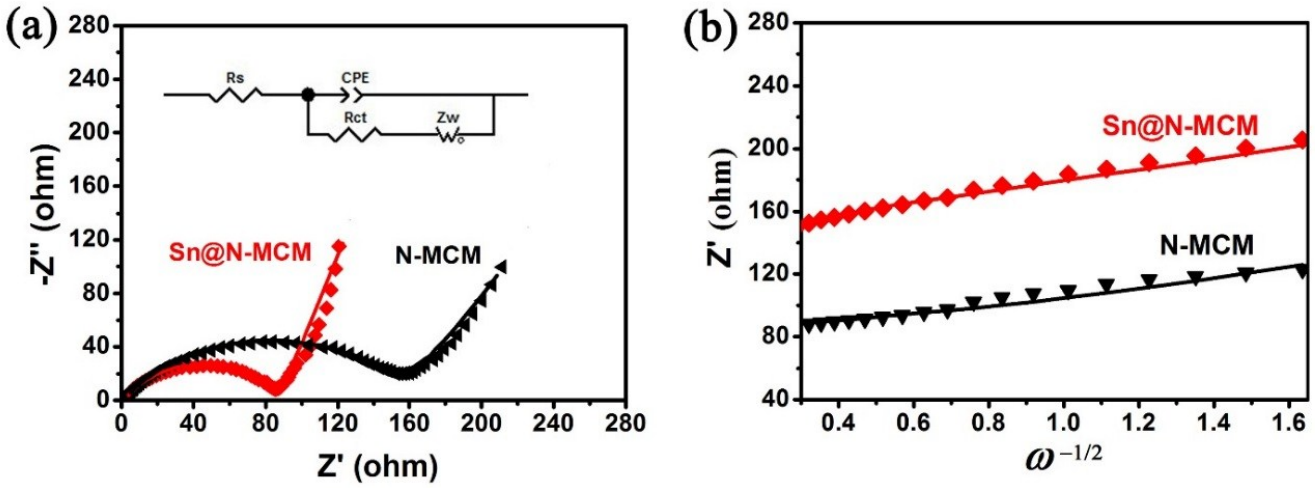


**Fig. S7.** (a) Nyquist plots of Sn@N-MCM and N-MCM electrodes and the corresponding simulated curves based on the equivalent circuit (inset). (b) Real parts of the impedance ($Z'$) versus the reciprocal square root of the angular frequency ($\omega$) in the low frequency region of the above Sn@N-MCM and N-MCM.

In this equivalent circuit, charge-transfer resistance ($R_{ct}$) is related to ability of charges transferring at electrode/electrolyte interfaces. Warburg impedance ($Z_w$) is associated with $Li^+$ ions diffusion in the Sn@N-MCM. In addition, $R_s$ stands for the solution resistance and constant-phase element (CPE) represents the double-layer capacitance.

The slope in equation (2) is Warburg factor ($\sigma$), which is an important parameter to calculate $Li^+$ diffusion coefficient ($D_{Li}$) using the equation (3):

$$Z' = R_D + R_L + \sigma\omega^{-1/2} \tag{2}$$

$$D_{Li} = \frac{R^2T^2}{2A^2n^4F^4C^2\sigma^2} \tag{3}$$

Where $R$ is the gas constant, $T$ is the absolute temperature, $A$ is the surface area of electrode, $n$ is the number of electrons per molecule during oxidization, $F$ is the Faraday constant, $C$ is the concentration of lithium ions.

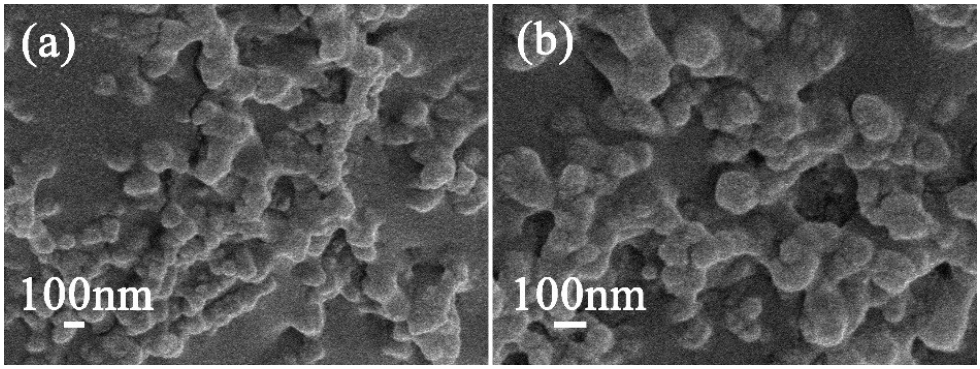


**Fig. S8.** SEM images of Sn@N-MCM electrode after 100 cycles at different magnifications.

.

**Table S1.** The content ratio of three N species in Sn@N-MCM.

| **N types** | pyridinic N | pyrrolic N | graphitic N |
|---|---|---|---|
| **Persentages** | 41.60% | 43.84% | 14.56% |

**Table S2.** Impedence parameters fitted from the equivalent circuit.

| **Samples** | $R_s(\Omega)$ | $R_{ct}(\Omega)$ | $\sigma$ |
|---|---|---|---|
| **Sn@N-MCM** | 1.71 | 86.29 | 27.57 |
| **N-MCM** | 1.11 | 161.20 | 39.60 |

**Table S3.** Comparison of the as-prepared Sn@N-MCM with previously reported Sn-based anodes for LIBs.

| Samples | Sn (wt%) | Rate capability | Cyclic stability | Ref. |
|---|---|---|---|---|
| Sn@N-MCM | 28.7% | 763.5 mA h $g^{-1}$ at 0.5 A $g^{-1}$<br>470.0 mA h $g^{-1}$ at 4 A $g^{-1}$<br>225.5 mA h $g^{-1}$ at 20 A $g^{-1}$ | 4 A $g^{-1}$/471 mA h $g^{-1}$/2500 th | This work |
| Sn@3D-NPC | 31.0% | 641 mA h $g^{-1}$ at 0.5 A $g^{-1}$<br>562 mA h $g^{-1}$ at 1 A $g^{-1}$<br>302 mA h $g^{-1}$ at 5 A $g^{-1}$ | 0.2 A $g^{-1}$/742 mA h $g^{-1}$ /200 th | 1 |
| Sn/C hybrid | 82.3% | 807 mA h $g^{-1}$ at 0.4 A $g^{-1}$<br>461 mA h $g^{-1}$ at 2 A $g^{-1}$ | 1 A $g^{-1}$/690 mA h $g^{-1}$/150 th | 2 |
| yolk–shell Sn@C | 70.0% | 720 mA h $g^{-1}$ at 0.5 A $g^{-1}$<br>580 mA h $g^{-1}$ at 1 A $g^{-1}$<br>350 mA h $g^{-1}$ at 5 A $g^{-1}$ | 0.2 A $g^{-1}$/810 mA h $g^{-1}$/500 th | 3 |
| Sn/CNT | 67.3% | 831 mA h $g^{-1}$ at 0.5 A $g^{-1}$<br>746 mA h $g^{-1}$ at 1 A $g^{-1}$<br>377 mA h $g^{-1}$ at 5 A $g^{-1}$ | 0.2 A $g^{-1}$/749 mA h $g^{-1}$/100 th | 4 |
| Sn@HC | 68.1% | 743 mA h $g^{-1}$ at 0.5 A $g^{-1}$<br>450 mA h $g^{-1}$ at 4 A $g^{-1}$<br>275 mA h $g^{-1}$ at 20 A $g^{-1}$ | 4 A $g^{-1}$/423 mA h $g^{-1}$/6000 th | 5 |
| Sn@NC | 59.0% | 1070 mA h $g^{-1}$ at 0.2 A $g^{-1}$<br>623 mA h $g^{-1}$ at 1 A $g^{-1}$<br>500 mA h $g^{-1}$ at 5 A $g^{-1}$ | 0.25 A $g^{-1}$/710 mA h $g^{-1}$/130 th | 6 |
| Sn@FLCNFs | 45.9% | 846 mA h $g^{-1}$ at 0.2 A $g^{-1}$<br>656 mA h $g^{-1}$ at 1 A $g^{-1}$ | 1 A $g^{-1}$/656 mA h $g^{-1}$/300 th | 7 |
| Sn@C | 45.7% | 672 mA h $g^{-1}$ at 0.2 A $g^{-1}$<br>205 mA h $g^{-1}$ at 16 A $g^{-1}$ | 4 A $g^{-1}$/410 mA h $g^{-1}$/4000 th | 8 |
| Sn@C | 63.0% | 778 mA h $g^{-1}$ at 0.5 A $g^{-1}$<br>336 mA h $g^{-1}$ at 8 A $g^{-1}$ | 1 A $g^{-1}$/691 mA h $g^{-1}$/500 th | 9 |
| Sn/C | 53.2% | 610.8 mA h $g^{-1}$ at 0.6 A $g^{-1}$<br>341.6mA h $g^{-1}$ at 6 A $g^{-1}$ | 3 A $g^{-1}$/537 mA h $g^{-1}$/1000 th | 10 |

## Supplemental References


1 Y. Guo, X. Zeng, Y. Zhang, Z. Dai, H. Fan, Y. Huang, W. Zhang, H. Zhang, J. Lu, F. Huo and Q. Yan, *ACS Appl. Mater. Interfaces*, 2017, **9**, 17172-17177.

2 F. Cheng, W.-C. Li, J.-N. Zhu, W.-P. Zhang and A.-H. Lu, *Nano Energy*, 2016, **19**, 486-494.

3 H. Zhang, X. Huang, O. Noonan, L. Zhou and C. Yu, *Adv. Funct. Mater.* , 2017, **27**, 1606023.

4 X. Zhou, L. Yu, X.-Y. Yu and X. W. Lou, *Adv. Energy Mater.*, 2016, **6**, 1601177.

5 N. Zhang, Y. Wang, M. Jia, Y. Liu, J. Xu, L. Jiao and F. Cheng, *Chem. Commun.*, 2018, **54**, 1205-1208.

6 C. Guo, Q. Yang, J. Liang, L. Wang, Y. Zhu and Y. Qian, *Mater. Lett.* , 2016, **184**, 332-335.

7 L. Qiao, L. Qiao, X. Li, X. Sun, H. Yue and D. He, *J. Mol. Sci.*, 2017, **52**, 6969-6975.

8 N. Zhang, Q. Zhao, X. Han, J. Yang and J. Chen, *Nanoscale*, 2014, **6**, 2827-2832.

9 Y. J. Hong and Y. C. Kang, *Small*, 2015, **11**, 2157-2163.

10 X. Huang, S. Cui, J. Chang, P. B. Hallac, C. R. Fell, Y. Luo, B. Metz, J. Jiang, P. T. Hurley and J. Chen, *Angew. Chem., Int. Ed.*, 2015, **54**, 1490-1493.